Model Based Ultrasonic Measurement Technique for Evaluation of the Adhesive Properties

Dobilas Liaukonis[1,2], Liudas Mazeika[2], Rimantas Barauskas[3], Audrius Neciunas[3]
[1]*Department of Electronics Engineering, Kaunas University of Technology, Studentu St. 50–338, LT-51368 Kaunas, Lithuania*
[2]*K. Barsauskas Ultrasound Institute, Kaunas University of Technology, K. Barsausko St. 59, LT-51423 Kaunas, Lithuania*
[3]*Department of Applied Informatics, Kaunas University of Technology, Studentu St. 50–407, LT-51368 Kaunas, Lithuania*
dobilas.liaukonis@ktu.lt

***Abstract*—The adhesive joints are common technique to joint different types of material such as metal to composite, composite to composite and etc. However, quality assessment of such joints is essentially more complicated comparing for to welds. Except problems related to presents of few materials with the completely different properties there is additional task of evaluation of the quality of cured adhesive. Usually joint defects are classified into the adhesive (bad adhesion between material and adhesive) and cohesive (defect in the layer of adhesive). Most of researcher's main attention is paying to the analysis of adhesive defects. Cohesive problem is more complicated and investigated essentially less. The key problem in this case is the fact that not some delamination should be detected, but the material properties of the thin layer of adhesive after curing should be evaluated.**

For solution of this task the model based ultrasonic measurement technique was proposed and investigated. According to this method, the frequency dependent attenuation is estimated and compared with attenuation obtained by Combined Maxwell and purely viscous model. The method was demonstrated investigating several samples of cured adhesive.

***Index Terms*—Adhesive bonds; Ultrasonic measurements; Volumetric viscosity; Numerical modelling.**

I. INTRODUCTION

Adhesive bonds are widely used to joint dissimilar materials such as metal to composite, aluminium plates to steel, metal to plastic and etc. Such joint types have several advantages including relative technological simplicity, as well as they are less affected by thermal strains. Adhesive bonding is widely used in vehicles manufacturing [1], aircraft industry [2], civil infrastructure such as bridges, buildings renovation or manufacturing instrumentality [3], [4]. Despite the advantages of widely used adhesives, they have drawbacks related to the need of surface preparation, necessity to avoid contaminations [5], time needed for curing the adhesive layer [6], aging and complexity of material characterization of the adhesive layer after gluing. The gluing defects can be divided into the two classes, such as adhesive and cohesive. Adhesive defects are defined as bad adhesion or delamination. The adhesive defects are mainly caused by human factors (contamination) and imperfections of gluing technology. This defect type is relatively easy to detect and is widely analysed by many researchers [7]–[11]. S. E. Hanneman and V. K. Kinra present technique which enables to assess quality of adhesive layer using low frequency ultrasonic waves with wavelength greater than the thickness of the layer. In this work the resonant methods are used [7]. In these works the attenuation of ultrasonic waves is investigated, however, physical properties of the adhesive such as volumetric viscosity is not determined. Castaings worked with EMAT transducer for detection of defect in lap-joints. It was shown that SH0 wave mode is highly sensitive to the quality of adhesive [8]. Heller investigated possibilities of laser ultrasonic technique for measurement of layer condition using Lamb waves [9]. Yang analysed vibration damping method for evaluation of whole layer condition [10]. Michael tested conventional reflection mode for assessment of the defect caused by the contamination in gluing of composite materials. [11]. Cohesive defects are defined as defects in the adhesive layer. Such defects are caused by non-suitable parameters or conditions of curing process or by bad quality of the adhesive itself. Detection of such defects is much more complicated as the properties of the thin layer of adhesive such as density, elasticity or volumetric viscosity needs to be characterized. There is a very limited set of methods suitable for solution of this task, and methods are base solution of an inverse problem [12].

Therefore, the objective of research presented was to develop ultrasonic technique for characterization of adhesive properties.

II. THE APPROACH USED FOR DETERMINATION OF THE PROPERTIES OF THE ADHESIVE

Evaluation of the parameters of the adhesive layer in the real objects is complicated, by the fact that even in the case of a single layer of adhesive it is surrounded from both sides

Manuscript received 14 March, 2018; accepted 15 June, 2018.

by the materials which were glued. So, in principle the direct access to adhesive is impossible for most measurement methods. Simultaneously, the results of measurements are essentially influenced by the surface roughness, thickness, non-homogeneity of the glued plates, the variation of the adhesive thickness, etc. The most important material parameters to be characterised are elastic properties of adhesive and volumetric viscosity, the values of which generally depend on the curing process. Most common and direct method for characterisation of such parameters is based on ultrasonic measurements. However, they enable to estimate the ultrasound velocity and attenuation of ultrasonic waves, but not physical parameters of material. On the other hand, the ultrasound velocity is determined by the material elastic properties and mass density. So, by means of appropriate methods these parameters can be reconstructed as long as the relation between ultrasonic wave velocity and elastic constants is strictly defined and known. The reconstruction of the volumetric viscosity is a more complicated task. There are no simple relations by using which the viscosity coefficient could be reconstructed from the measured attenuation of ultrasonic waves. It is necessary to take into account that in the case of adhesives the attenuation is frequency dependent. Therefore, for estimation of the volumetric viscosity coefficient the model based measurement approach should be used.

In order to investigate the possibilities of such an approach the separate sample of the cured adhesive has been investigated by using the measurement set-up presented in Fig. 1. The ultrasonic transducer was attached to the sample of the adhesive by using the buffer (plexiglas) rod. The buffer rod is used for determination of the reference signal, as well as a material with known properties for determination of the reflection and transmission coefficients between the buffer rod and adhesive under investigation.

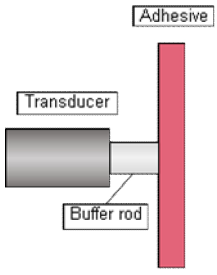

Fig. 1. The set up for determination of the adhesive properties.

The transducer is excited by a short pulse, and several reflections of the signal are obtained Fig. 2. By assuming that the frequency spectrum of the incident signal generated into the buffer rod is $U_{in}(f)$, then the frequency spectrum of the signal reflected at the end of the buffer rod will be

$$U_{\text{plex}}(f) = U_{\text{in}}(f) \times H_{\text{plex}}\left(f, d_{\text{plex}}\right) \times K_{\text{R,plex-adh}}, \quad (1)$$

where $K_{\text{R,plex-adh}} = \dfrac{z_{\text{adh}} - z_{\text{plex}}}{z_{\text{adh}} + z_{\text{plex}}}$ is the reflection coefficient from the boundary plexiglas adhesive; $z_{\text{adh}} = \rho_{\text{adh}} \times c_{\text{adh}}$ and $z_{\text{plex}} = \rho_{\text{plex}} \times c_{\text{plex}}$ are acoustic impedances of the adhesive and plexiglas; $\rho_{\text{adh}}, c_{\text{adh}}$, $\rho_{\text{plex}}, c_{\text{plex}}$ are the mass densities and ultrasound velocities of adhesive and Plexiglas correspondingly; $H_{\text{plex}}\left(f, d_{\text{plex}}\right)$ is frequency and thickness dependent transfer function of plexiglas. It is also assumed that reflection coefficient is not frequency dependent and d_{plex} is the length of the plexiglas rod. As the attenuation in the plexiglas is not so strongly dependent on frequency as in the adhesive the frequency spectrum $U_{\text{plex}}(f)$ was used as the reference.

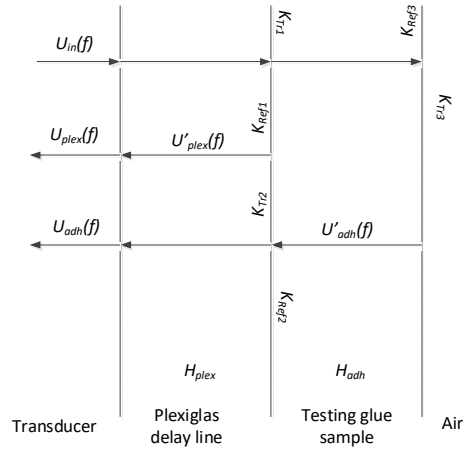

Fig. 2. Explanation of the reflections taking place according measurement set-up.

The frequency spectrum of the signal reflected by the back wall of the adhesive is expressed by

$$U_{\text{adh}}(f) = U_{\text{in}}(f) \times H_{\text{plex}}\left(f, d_{\text{plex}}\right) \times K_{\text{T,plex-adh}} \times \times K_{\text{T,adh-plex}} \times H_{\text{adh}}\left(f, d_{\text{adh}}\right), \quad (2)$$

where $K_{\text{T,plex-adh}} = \dfrac{2z_{\text{adh}}}{z_{\text{adh}} + z_{\text{plex}}}$ and $K_{\text{T,adh-plex}} = \dfrac{2z_{\text{plex}}}{z_{\text{adh}} + z_{\text{plex}}}$ are the transmission coefficient from the boundary plexiglas-adhesive and adhesive-plexiglas; $H_{\text{adh}}\left(f, d\right)$ is frequency and thickness dependent transfer function of adhesive. This transfer function can be obtained from the ration of spectra $U_{\text{adh}}(f)$ and $U_{\text{plex}}(f)$

$$\frac{U_{\text{adh}}(f)}{U_{\text{plex}}(f)} = \frac{U_{\text{in}}(f) \times H_{\text{plex}}\left(f, d_{\text{plex}}\right) \times K_{\text{T,plex-adh}} \times}{U_{\text{in}}(f) \times H_{\text{plex}}(f, 2d) \times} \frac{\times K_{\text{T,adh-plex}} \times H_{\text{adh}}\left(f, d_{\text{adh}}\right)}{\times K_{\text{R,plex-adh}}}, \quad (3)$$

where d_{adh} is the thickness of the adhesive. It can be shown that

$$H_{\text{adh}}\left(f, d_{\text{adh}}\right) = \frac{z_{\text{adh}} - z_{\text{plex}}}{4 z_{\text{adh}} z_{\text{plex}}} \times \frac{U_{\text{adh}}(f)}{U_{\text{plex}}(f)}. \quad (4)$$

It can be seen that the transfer function of the adhesive

can be determined from this equation only in the case if densities and ultrasound velocities of both materials are known. It can be assumed that the density for particular adhesive is known or at least can be measured using independent methods. The ultrasound velocity can be measured by measuring the delay time between the signal reflected from the back wall at time moment t_{adh} of the sample and the signal reflected from the boundary plexiglas-adhesive at time moment t_{plex}

$$c_{\text{adh}} = \frac{2 \times d_{\text{adh}}}{t_{\text{adh}} - t_{\text{plex}}}, \tag{5}$$

where d_{adh} is the thickness of the adhesive. After determination of ultrasound velocity and mass density of the adhesive the attenuation was estimated as

$$A_{\text{adh}}\left(f, d_{\text{adh}}\right) = 1 / H_{\text{adh}}\left(f, d_{\text{adh}}\right). \tag{6}$$

The experimentally determined attenuation was approximated by using the following dependency [13]

$$A'_{\text{adh}}\left(f, d_{\text{adh}}\right) = \mathrm{e}^{\alpha_{\text{adh}} 2\pi f^2 d_{\text{adh}}}, \tag{7}$$

where attenuation coefficient α_{adh} is obtained by solving optimisation problem

$$\alpha_{\text{adh}} = \arg\left\{\min_{\alpha_{\text{adh}}}\left[\left|A'_{\text{adh}}\left(f, d_{\text{adh}}\right) - A_{\text{adh}}\left(f, d_{\text{adh}}\right)\right|\right]\right\}. \tag{8}$$

The second stage of the measurement technique is the reconstruction of the both elastic properties and volumetric viscosity by fitting experimentally determined transfer function with the transfer function obtained by using computer modelling. For this purpose, the finite element model was developed.

The finite element model for the shear wave propagation is based on the combined Maxwell and purely viscous model, the finite element of which is represented Fig. 3. The full strain of the element is $\boldsymbol{\varepsilon}$. In the Maxwell part of the model the strain component $\boldsymbol{\varepsilon}_{\text{d}\mu}$ presents the relaxation component. In a steady state condition $\boldsymbol{\varepsilon}_{\text{d}\mu}$ tends to vanish during time. However, during the transient wave processes it can be interpreted as an additional degree of freedom within the element, which may influence the overall damping behaviour of the model.

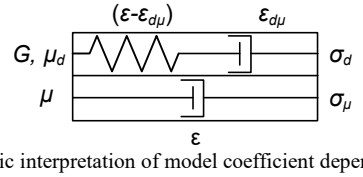

Fig. 3. Schematic interpretation of model coefficient dependence.

The finite element equation system reads as:

$$\begin{cases} \mathbf{M}\ddot{\mathbf{U}}^e = -\mathbf{K}^e\mathbf{U}^e - \mathbf{C}^e\dot{\mathbf{U}} + \boldsymbol{\Psi}^e, \\ \tau\dot{\boldsymbol{\varepsilon}}^e_{d\mu} = \mathbf{B}^e\mathbf{U}^e - \boldsymbol{\varepsilon}^e_{d\mu}, \end{cases} \tag{9}$$

where the first equation is the structural dynamic equation in terms of nodal displacements $\mathbf{U}^e$, and the second equation describes the time behaviour of the relaxation strains within each element of the waveguide structure.

In (9) the matrices are determined as:

$$\begin{cases} \mathbf{K}^e = G \int\limits_{V^e} \mathbf{B}^{eT}\mathbf{B}^e dV, \\ \mathbf{C}^e = \mu \int\limits_{V^e} \mathbf{B}^{eT}\mathbf{B}^e dV, \\ \boldsymbol{\Psi}^e = G \int\limits_{V^e} \sum\limits_{i=1}^{n} \mathbf{B}^{eT}\boldsymbol{\varepsilon}^e_{d\mu} dV, \end{cases} \tag{10}$$

where matrix $\mathbf{K}^e$ is the stiffness matrix determined by shear modulus G of the material, $\mathbf{C}^e$ is the damping matrix of the purely viscous part of the model determined by viscosity coefficient μ, $\boldsymbol{\Psi}^e$ nodal force vector, which simulates the strain relaxation behaviour in the course of time and matrix $\mathbf{B}^e$ is the strain matrix of the element.

In this model the damping properties are given as the combination of values of damping coefficient μ and relaxation time $\tau = \frac{\mu_d}{G}$.

Element equations (9), (10) assembled to structural equations read as:

$$\begin{cases} \mathbf{M}\ddot{\mathbf{U}} = -\mathbf{K}\mathbf{U} - \mathbf{C}\dot{\mathbf{U}} + \mathbf{K}_u\boldsymbol{\varepsilon} + \mathbf{F}, \\ \tau\mathbf{I}\dot{\boldsymbol{\varepsilon}} = E_u\mathbf{U} - \boldsymbol{\varepsilon}, \end{cases} \tag{11}$$

where structural strains vector $\boldsymbol{\varepsilon}$ contains the relaxation strains $\boldsymbol{\varepsilon}^e_{du}$ of all elements of the structure, E_u, $\mathbf{K}_u$ are the corresponding matrices obtained during the assembly operation and $\mathbf{F}$ is nodal force vector representing the external excitation.

Equation (11) is the full model equation on the base of which the dynamic properties of the waveguide may be investigated. At given excitation, direct time integration of (11) provides the time laws of displacements and velocities of all nodes of the model taking place due to the propagating wave. The Fourier analysis of the obtained time laws provides the frequency components of the signal.

Simultaneously, by assuming $\mathbf{F} = 0$ the complex eigenvalue problem can be formulated as

$$\lambda\begin{bmatrix} \mathbf{I} & 0 & 0 \\ 0 & \mathbf{I} & 0 \\ 0 & 0 & \mathbf{I} \end{bmatrix}\begin{Bmatrix} \mathbf{U} \\ \mathbf{V} \\ \boldsymbol{\varepsilon} \end{Bmatrix} + \begin{bmatrix} 0 & -\mathbf{I} & 0 \\ \mathbf{M}^{-1}\mathbf{K} & \mathbf{M}^{-1}\mathbf{C} & -\mathbf{M}^{-1}\mathbf{K}_u \\ -\frac{1}{\tau}\mathbf{I}E_u & 0 & \frac{1}{\tau}\mathbf{I} \end{bmatrix}\begin{Bmatrix} \mathbf{U} \\ \mathbf{V} \\ \boldsymbol{\varepsilon} \end{Bmatrix} = 0. \tag{12}$$

Negative real parts of eigenvalues $\mathrm{Re}(\lambda_i)$ are the attenuation factors at frequencies, which are equal to the corresponding complex parts $\mathrm{Im}(\lambda_i)$ of the same eigenvalues.

III. The Approach Used for Determination of the Properties of the Adhesive

The experiment was carried out in accordance with the set-up presented in Fig. 1. The flat CX-165 10 MHz transducer was used for generation and reception of ultrasonic waves. For excitation of the transducer and acquisition of the signals, the ultrasonic system developed by Ultrasound Research Institute in Kaunas University of technology was used. The transducer has been excited with 50 ns electrical rectangular pulse. Investigations have been performed on the cured sample of structural the Young's modulus of which is E = 1700 MPa. The sample presented in Fig. 4 was investigated. The thickness of the sample was d_{adh} = 4.06 ± 0.01 mm. The measured mass density of the sample was 1160 kg/m^3. The contact gel was used to obtain the necessary acoustic coupling.

Fig. 4. The photo of the sample.

The measured signals are presented in Fig. 5. The reflections from the boundary plexiglas-adhesive and from the backwall of the adhesive can be observed clearly. Both reflections were separated by using time windows. The corresponding frequency spectra are presented in Fig. 6 where the spectrum of the signal reflected by the backwall of the adhesive has a much lesser frequency bandwidth. However, within this bandwidth the amplitude of the spectrum is higher as the reflection and transmission coefficients were not considered. In order to take in to account these coefficients the ultrasound velocity in the adhesive and the acoustic impedance should be estimated.

The ultrasound velocity in the adhesive sample was obtained by measuring the time of flight t_{PA} between signals reflected by boundary plexiglas-adhesive and the adhesive backwall reflection (Fig. 7). The delay time difference was estimated using cross correlation as

$$X_{PA}(t_m) = \sum_{k=0}^{M-1} u_A(t_k) \times u_P(t_m - t_k), \qquad (13)$$

where $m = 0 \div M-1$; M is the total number of samples in the signals; $u_A(t_k)$ and $u_P(t_k)$ are the signals reflected by the backwall of adhesive and by the boundary plexiglas-adhesive correspondingly.

The approximate value of the delay time t'_{PA} was obtained as maximum position in cross-correlation function

$$t_{\max} = \arg\left[\max_t \left(X_{PA}(t_m)\right)\right]. \qquad (14)$$

In order to obtain more accurate delay time estimation with subsample accuracy the cosine interpolation function [14]

$$t_{ss} = \frac{\theta}{f_s \times \omega_0}, \qquad (15)$$

was used, where f_s, is the sampling frequency, $\omega_0 = \arccos\left[\frac{u(t_{ss-1}) + u(t_{ss+1})}{2u(t_{ss})}\right]$ the centre angular frequency of the signal and $\theta = \arctan\left[\frac{u(t_{ss-1}) + u(t_{ss+1})}{2u(t_{ss}) \times \sin(\omega_0)}\right]$ is the phase [15].

Finally, the precise time of flight value is obtained by

$$t_{PA} = t_{\max} + t_{ss}. \qquad (16)$$

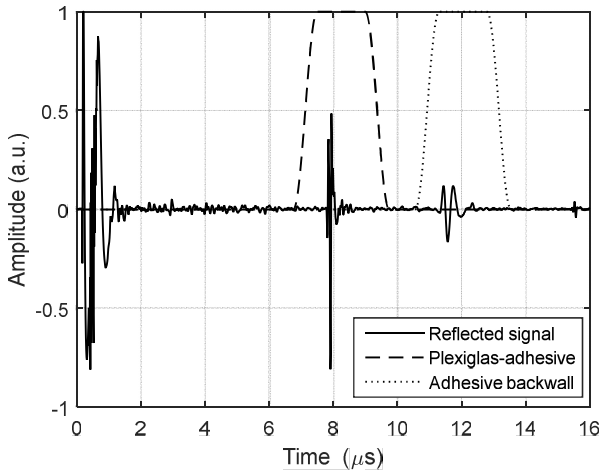

Fig. 5. Ultrasonic signal measured on the sample.

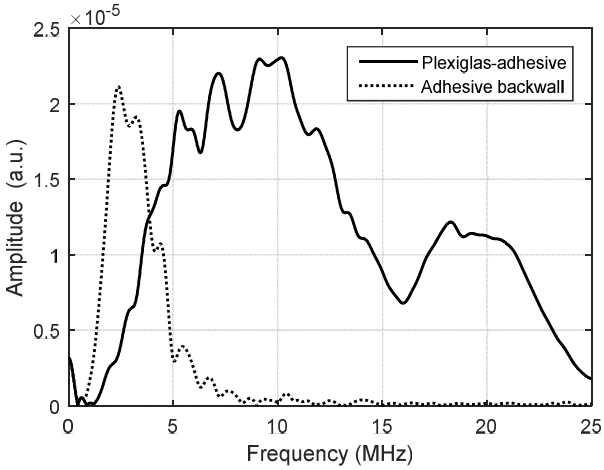

Fig. 6. Frequency spectra of the signals reflected by boundary plexiglas – adhesive and backwall of adhesive. Doted line is adhesive backwall, solid line is plexiglas (buffer) reflection.

The ultrasound velocity the adhesive is obtained as

$$c_{\mathrm{adh}} = \frac{d_{\mathrm{adh}}}{t_{PA}}. \qquad (17)$$

Then the impedance of adhesive is calculated and corrected spectrum of the signal reflected by the backwall of

the adhesive is estimated as

$$U'_{\text{adh}}(f) = \frac{z_{\text{adh}} - z_{\text{plex}}}{4 z_{\text{adh}} z_{\text{plex}}} \times U_{\text{adh}}(f). \quad (18)$$

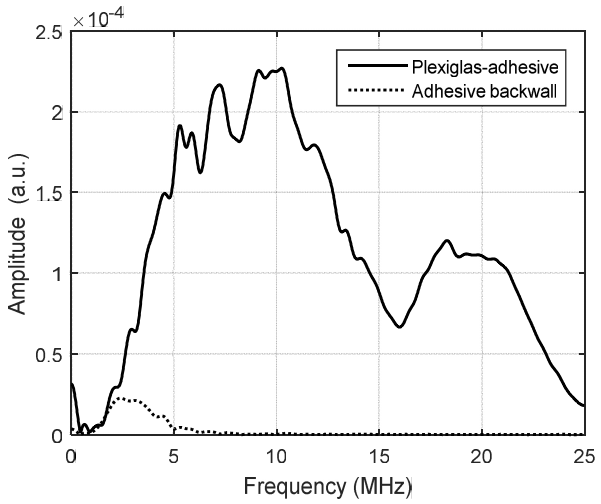

Fig. 7. Frequency spectrum of the signals reflected by boundary plexiglas – adhesive and the modified spectrum of the backwall reflection.

Finally, the attenuation dependence on frequency reads as follows

$$H_{\text{adh}}(f, d_{\text{adh}}) = \frac{U'_{\text{adh}}(f)}{U_{\text{plex}}(f)}. \quad (19)$$

The obtained dependency (19) is presented in Fig. 8. The approximation calculated by (7) is also presented in the same figure. Attenuation coefficient $\alpha_{\text{adh}} = -2.56$ is obtained by (8). The material viscosity characteristics of the adhesive are frequency dependent. At pulse duration $T_{exc} = 0.1\mu s$ the values of the attenuation constants of the adhesive were obtained by selecting an optimum combination of values of stiffness-proportional damping coefficient μ and the Maxwell model relaxation constant τ, which provide the best fit between the experimental and computed results. The following results were obtained:

For shear wave propagation the shear modulus value was known as

$$G = 4.788e9(1-\sigma)/((1+\sigma)(1-2\sigma)) = 7.074\times10^9\, N/m^2$$

where $\sigma = 0.333$ is the Poisson's ratio and mass density is $\rho = 1420 kg/m^3$, $T_{exc} = 0.1\mu s$, stiffness-proportional damping matrix was, $C = \frac{\mu}{E_{eqv}} K$, and the relaxation constant τ of the Maxwell viscosity model was used.

The computational modelling was carried out by using the model of similar but not identical set-up as in the experiment. The model was based on (9)–(11). Only propagation of ultrasonic waves in the adhesive sample was simulated. The plexiglas rod was not included into the model just in order simplify solutions analysis and to avoid possible inadequacies of the model to reality at the junctions between the two zones. The 1D model described in previous section was used. The excitation was performed using burst with Gaussian envelope with central frequency 5.5 MHz and 60 % bandwidth. The modelled signals in the time domain are presented in Fig. 9. Simulation was performed many times with different viscosity constants of the model, by attempting to tune the computed results to experimental ones. Our experiments revealed that the obtained best combination of values μ = 8.5 N/m^2 and $\tau = \frac{\mu_d}{G} = 22.3$ T_{exc} could be determined rather unambiguously. The signals and frequency spectra obtained after such viscosity parameter tuning are presented in Fig. 9 and in Fig. 10.

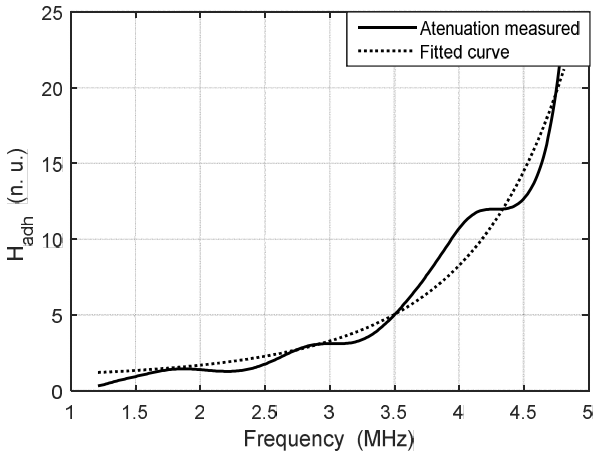

Fig. 8. Experimentally determined attenuation in adhesive sample versus frequency (equal line) and approximation according (7) (dotted line).

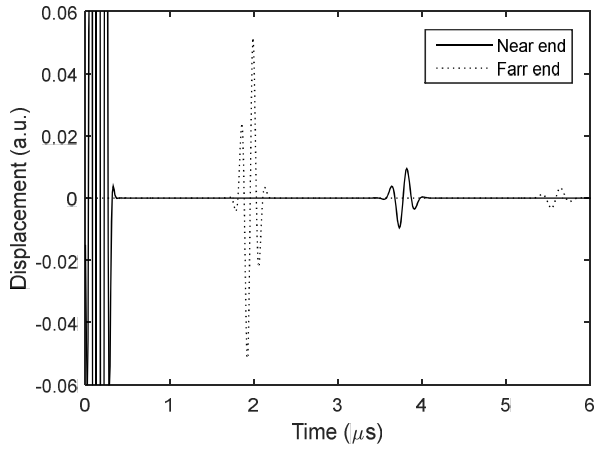

Fig. 9. The signals obtained by modelling after viscosity parameter tuning.

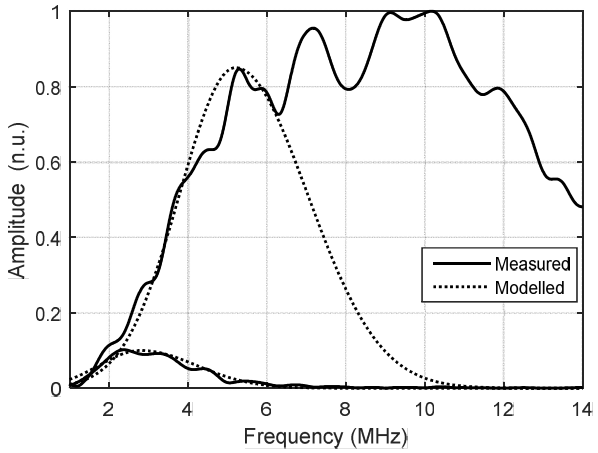

Fig. 10. The comparison of frequency spectra of the modelled signals and measured data (equal line measured, dotted line modelled).

The good coincidence of the spectra can be observed. The attenuation curve in the adhesive sample was obtained by solving (12). The modelled curve presented in Fig. 11 is based on points, the ordinates of which are negative real parts of eigenvalues $\mathrm{Re}(\lambda_i)$ and the abscissas are the frequencies $\mathrm{Im}(\lambda_i)$ of the corresponding eigenvalues.

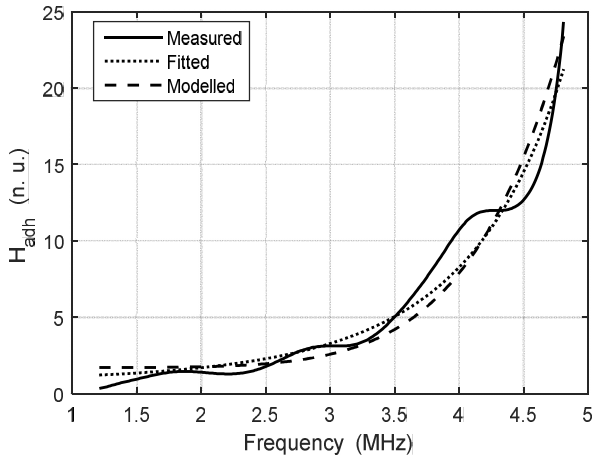

Fig. 11. Experimentally determined attenuation in adhesive sample versus frequency (equal line) and approximation according (7) (dotted line), modelled (dashed line).

Again, the match between computation and experiment is good as can be seen from Fig. 11 by comparing the "fitted" and "modelled" curves.

IV. CONCLUSIONS

The ultrasonic measurement technique for assessment of the properties of adhesive has been proposed and investigated. The technique is based on measurements of ultrasound velocity and frequency dependent attenuation which is related to the volumetric viscosity using finite element modelling. The numerical model is obtained by combining Maxwell and purely viscous material approaches. It has been demonstrated that the selected viscosity model characterized by two parameters as damping constant and relaxation time is sufficient for the characterization of the material viscosity properties as a good match between the computed and experimental results was demonstrated. Obviously, the viscosity constants are frequency dependent, therefore a series of experiments over a certain range of central excitation frequency values of Gaussian envelope would be necessary for the complete characterization of the material.

REFERENCES

[1] T. A. Barnes, I. R. Pashby, "Joining techniques for aluminium spaceframes used in automobiles Part II - adhesive bonding and mechanical fasteners", *Journal of Materials Processing Technology*, vol. 99, pp. 72–79, 2000. DOI: 10.1016/S0924-0136(99)00361-1.

[2] A. Higgins, "Adhesive bonding of aircraft structures", *International Journal of Adhesion & Adhesives*, vol. 20, pp. 367–376, 2000. DOI: 10.1016/S0143-7496(00)00006-3.

[3] V. M. Karbhari, L. Zhao, "Use of composites for 21st century civil infrastructure", *Computer Methods in Applied Mechanics, and Engineering*, vol. 185, pp. 433–454, 2000. DOI: 10.1016/S0045-7825(99)90270-0.

[4] L. V. D. Einde, L. Zhao, F. Seible, "Use of FRP composites in civil structural applications", *Construction and Building Materials*, vol. 17, pp. 389–403, 2003. DOI: 10.1016/S0950-0618(03)00040-0.

[5] D. Liaukonis, "Ultrasonic imaging of adhesive bond contamination", in *Proc. 20th Int. Conf. Electronics*, 2016.

[6] L. Svilainis, A. Rodriguez, D. Liaukonis, A. Chaziachmetovas, "Assessment of ultrasound velocity application for chemical process monitoring", *Elektronika ir Elektrotechnika*, vol. 21, no. 4, pp. 50–55, 2016. DOI: 10.5755/j01.eee.21.4.12783.

[7] S. E. Hanneman, V. K. Kinra, "A new technique for ultrasonic nondestructive evaluation of adhesive joints: Part I. Theory", *Experimental Mechanics*, vol. 32, pp. 323–331, 1992. DOI: 10.1007/BF02325585.

[8] M. Castaings, "SH ultrasonic guided waves for the evaluation of interfacial adhesion", *Ultrasonics*, vol. 54, pp. 1760–1775, 2014. DOI: 10.1016/j.ultras.2014.03.002.

[9] K. Heller, L. J. Jacobs, J. Qu, "Characterization of adhesive bond properties using Lamb waves", *NDT&E International*, vol. 33, pp. 555–563, 2000. DOI: 10.1016/S0963-8695(00)00022-0.

[10] S. Yang, L. Gu, R. F. Gibson, "Nondestructive detection of weak joints in adhesively bonded composite structures", *Composite Structures*, vol. 51, pp. 63–71, 2001. DOI: 10.1016/S0263-8223(00)00125-2.

[11] M. Wood, P. Charlton, D. Yan, "Ultrasonic evaluation of artificial kissing bonds in CFRP composites", *The e-Journal of Nondestructive Testing*, vol. 19, pp. 1–10, 2014.

[12] E. Siryabe, M. Renier, A. Meziane, J. Galy, M. Castaings, "Characterization of cohesive and adhesive properties of adhesive bonds using transmitted ultrasonic waves", in *Conf. Rec. 19th (WCNDT 2016)*, Munich, 2016.

[13] Ping He, "Simulation of ultrasound pulse propagation in lossy media obeying a frequency power law", *IEEE Trans. Ultrasonics, Ferroelectrics, and Frequency Control*, vol. 45, pp. 114–125, 1998. DOI: 10.1109/58.646916.

[14] I. Cespedes, *et al*., "Methods for estimation of subsample time delays of digitized echo signals", *Ultrasonic Imaging*, vol. 17, pp. 142–171, 1995. DOI: 10.1177/016173469501700204.

[15] L. Svilainis, *et al*., "Subsample interpolation bias error in time of flight estimation by direct correlation in digital domain", *Measurement*, vol. 46, pp. 3950–3958, 2013. DOI: 10.1016/j.measurement.2013.07.038.